0.1 Introduction

Using causality

As noted above, when the vertical distance between the source and receiver goes to zero, the wavenumber integration for the direct arrival is difficult because the upper limit of integration cannot be easily truncated because of the lack of a decaying exponential term as k increases. Recent papers on modeling the ambient noise H/V ratio in the frequency domain (Sánchez-Sesma et al., 2011) have focused on the imaginary part of the Green's function which leads to the approach described here.

Real time series have the property $h(t) \Leftrightarrow R_e(\omega) + iI_o(\omega)$, where the e and o subscripts indicate even and odd functions of angular frequency, respectively. A time series can be expressed as $h(t) = h_e(t) + h_o(t)$ and if $h(t)$ is real, then $h_e(t) \Leftrightarrow R_e(\omega)$ and $h_o(t) \Leftrightarrow iI_o(\omega)$. If $h(t)$ is causal, e.g., $h(t) = 0$ for $t < 0$, then for $t > 0$, $h_e(t) = h_o(t) = \frac{1}{2}h(t)$.

For a real causal time function, Papoulis (1962) (§10-2) shows that the real and imaginary parts of $H(\omega)$ are related by Hilbert transforms

$$I_o(\omega) = -\frac{1}{\pi}\int_{-\infty}^{\infty}\frac{R_e(\Omega)}{\omega-\Omega}d\Omega \qquad R_e(\omega) = \frac{1}{\pi}\int_{-\infty}^{\infty}\frac{I_o(\Omega)}{\omega-\Omega}d\Omega + R(\infty)$$

where the $R(\infty)$ term arises from the behavior of $h(t)$ at $t = 0$. These relations are obtained using the convolution theorem in the frequency domain, $g(t)h(t) \Leftrightarrow \frac{1}{2\pi}\int_{-\infty}^{\infty} G(\Omega)H(\omega-\Omega)d\Omega$, together with $g(t) = U(t)$, the unit step function, and its Fourier transform (Table **??**).

The unit step function can be used to recover the causal $h(t)$ for $t > 0$ from the even and odd parts of the function as follows:

$$h(t) = U(t)2h_e(t) = U(t)\frac{1}{2\pi}\int_{-\infty}^{\infty}2R_e(\omega)e^{i\omega t}d\omega = U(t)\frac{1}{2\pi}\int_{-\infty}^{\infty}2\,\mathrm{Re}[H(\omega)]e^{i\omega t}d\omega \tag{0.1.1a}$$

$$h(t) = U(t)2h_o(t) = U(t)\frac{1}{2\pi}\int_{-\infty}^{\infty}2iI_o(\omega)e^{i\omega t}d\omega = U(t)\frac{1}{2\pi}\int_{-\infty}^{\infty}2i\,\mathrm{Im}[H(\omega)]e^{i\omega t}d\omega \tag{0.1.1b}$$

Note the first relation can define $h(t)$ at $t = 0$, while the second cannot.

In cylindrical coordinates the frequency domain representation of the Green's function requires the evaluation of an integral of the form $\int_0^{\infty} F(k,\omega)J_n(kr)kdk$. Recall that the $F(k,\omega)$ for the Sommerfeld integral, $F(k,\omega) = e^{-\nu|z|}/\nu$, is complex for $k < \omega/V$ and real for $k > \omega/V$. When time-domain damping is introduced to avoid Discrete Fourier Transform periodicity and singularities due to complex poles of $F(k,\omega)$ in general media by replacing ω with $\omega - i\alpha$, then $F(k,\omega - ia)$ is complex for all k, but is effectively real for large k compared to ω/V. Thus the $Im[H(\omega)]$ in (0.1.1b) might be expressed as $Im[H(\omega)] = \int_0^{k_{max}} Im[F(k,\omega - ia)]J_n(kr)kdk$.

The k_{max} upper integration limit is not a function of the vertical distance z between the source and the observation point, which would be the case for the integral $\int_0^{k_{max}} F(k, \omega - ia) J_n(kr) k dk$.

This suggests the following algorithm for use with the Discrete Fourier transform:

Table 1 Algorithm for approximate integration

Define sample interval Δt to set highest frequency
Define number of points in time series N
Define a $k_{max} = FAC * \omega / V_{min}$ with $FAC > 1$
Apply the approximate wavenumber integration using $2N$ points
Apply the inverse 2N Fourier transform and use only first N points

To illustrate this procedure, the RDD Green's functions are computed for the single layer over a halfspace SCM model of Table **??** using the parabolic source pulse with a duration of 0.5s. The left frame of Figure 1 illustrates the fact that this technique creates an odd function with respect to the origin time. The right frame shows that when the traces are windowed to include just positive times, there is good agreement with the Green's functions obtained by evaluating $\int_0^{\infty} F(k, \omega) J_n(kr) k dk$, except at the shortest distance where the forward and reverse propagating signals interfere. In these plots $\Delta t = 0.05$s and the time series were N=512 and N=256 samples long. The a parameter in $\omega - ia$ was set to a small value that $aN\Delta t = 0.1$ to be able to display the odd function with respect to the origin time.

Figure 2 compares the synthetics for a value of $a = 2.5/(N\Delta t)$ with the first time point representing a travel time of $r/6.0 - 2.0$s. The effect of this time shift is to move the negative time arrivals of Figure 1 to the end of the $2N$ long trace. The required operation of (**??**) then enhances that part of the traces, leading to the large signal at the end of the trace at a distance of 35km after the $2N$ long time series is cut to display the first N points. Thus additional care is required using this approach.

In addition to addressing the problematic case of the source and receiver at the same depth, (0.1.1b) can also be used to model the autocorrelation of a component of displacement caused by ambient noise. In the frequency domain this permits modeling the H/V ratio (Sánchez-Sesma et al., 2011; Perton et al., 2020) and in the time domnain, deeper reflections observed by Tibuleac and von Seggern (2012).

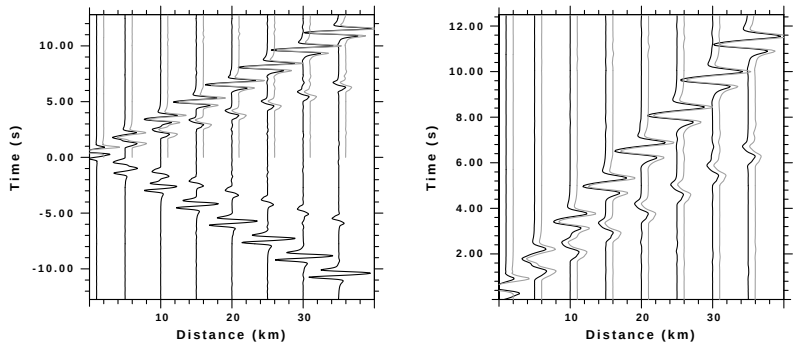

Figure 1 Comparison of the RDD Green's function at the surface ($z = 0$) for a source at a depth of $h = 1.0$ km in the SCM model of Table **??**. Left) comparison of computations. Right) plot of the first 12.5s of the synthetic. In these figures the solid black and gray traces are the result of integrating $ImF(k, \omega - ia)$ and $F(k, \omega - ia)$, respectively and start 12.5s before the origin time and at the origin time, respectively. For ease of comparison, the gray traces are shifted 1 km to the right. Trace amplitude have been scaled to correct for $1/r$ geometrical spreading.

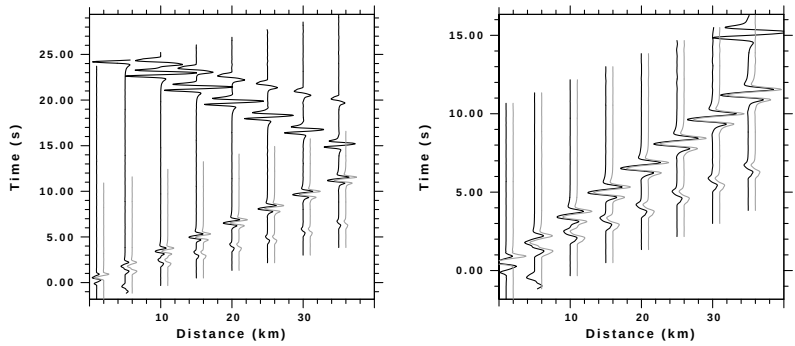

Figure 2 Comparison of the RDD Green's function at the surface ($z = 0$) for a source at a depth of $h = 1.0$ km in the SCM model of Table **??** when the first sample is the reduced travel time of $r/6.0 - 2$ seconds after the origin time. The description of traces is the same as in Figure 1.

Bibliography

Papoulis, A. (1962). *The Fourier Transform and its Applications*. McGraw Hill, New York.

Perton, M., Spica, Z. J., Clayton, R. W., and Beroza, G. C. (2020). Shear wave structure of a transect of the los angeles basin from multimode surface waves and H/V spectral ratio. *Geophys. J. Int.*, 220:415–427.

Sánchez-Sesma, F. J., Rodríguez, M., Iturrarán-Viveros, U., Luzón, F., Campillo, M., Margerin, L., García-Jerez, A., Suarez, M., Santoyo, M. A., and Rodríguez-Castellanos, A. (2011). A theory for microtremor H/V spectral ratio: application for a layered medium:. *Geophy. J. Inte.*, 186:221–225.

Tibuleac, I. M. and von Seggern, D. (2012). Crust-mantle boundary reflectors in Nevada from ambient seismic noise autocorrelations: Crust-mantle boundary reflectors in Nevada. *Geophysical Journal International*, 189:493–500.